

A LARGE PHOTODISSOCIATION REGION AROUND THE COLD, UNUSUAL CLOUD G216–2.5

JONATHAN P. WILLIAMS¹

Radio Astronomy Laboratory, University of California, Berkeley, Berkeley, CA 94720

AND

RONALD J. MADDALENA

National Radio Astronomy Observatory,² Green Bank, WV 24944

Received 1995 June 23; accepted 1996 January 5

ABSTRACT

Observations are presented of an atomic cloud that we contend links a non–star-forming giant molecular cloud discovered by Maddalena & Thaddeus to two separate regions of OB star formation each over 50 pc away. The maps suggest that the cloud is a part of a larger molecular complex that has been partially photodissociated by these stars. The association of the cloud with stars of known spectral type allows a more definitive estimate of its heliocentric distance, 2.3 kpc. The precise amount of H I that is associated with the molecular gas is highly uncertain because of the ubiquity of emission along the line of sight, but it is argued that it may possess a large envelope (as seen around other molecular clouds) of mass $\sim 10^6 M_{\odot}$, and that the mass of photodissociated gas due to the nearby OB stars is only a small fraction of this, $\sim 10^5 M_{\odot}$. The molecular cloud itself is gravitationally bound, but the atomic cloud (whatever its mass) is unbound and probably evaporating into the general interstellar medium. The two sites of star formation that are most likely to have caused the photodissociation are S287 (an H II region dominated by an O9.5 V star) and a second, unidentified H II region with a infrared luminosity of $1.1 \times 10^4 L_{\odot}$. However, the incident flux on the molecular cloud due to these H II regions is extremely weak and appears to be no more than the average Habing value, i.e., $G_0 \simeq 1$, implying that the current rate of dissociation is small. The implications of these observations for diverse arguments concerning the evolutionary state of this cloud is discussed.

Subject headings: ISM: clouds — ISM: H II regions — ISM: molecules —
 open clusters and associations: general — stars: formation

1. INTRODUCTION

The observations of Maddalena & Thaddeus (1985, hereafter Paper I) of a large, cold molecular cloud in the outer Galaxy with no obvious signs of associated star formation have provoked much interest in recent years. The discoverers suggested that the cloud may have recently formed, that star formation might soon begin, and that the cloud would then take on the appearance of a more typical Orion-like object. This was the hypothesis adopted by Williams, de Geus, & Blitz (1994) in their study of the clumpy structure of the cloud. However, Lee, Snell, & Dickman (1991, 1994) suggested, on the contrary, that the cloud is the remnant from a past episode of massive star formation on the basis of kinematics (the existence of shells and large scale velocity gradients across the cloud) and the discrepancy between its virial and luminous mass.

Almost all molecular clouds that have been mapped and studied in detail are found to contain young stellar objects that are seen most clearly in the infrared (Myers et al. 1986). Large-scale CO surveys have reported the existence of cold clouds that appear to possess some of the properties of the Maddalena & Thaddeus cloud (hereafter G216–2.5): low peak temperatures, large line widths, and lack of optical, radio, and infrared counterparts (Solomon, Sanders, & Rivolo 1985; Mooney & Solomon 1988). However, such

clouds are distant, and the sensitivity of the radio and infrared surveys is too low to rule out the existence of relatively large amounts of associated star formation (Blitz 1993). G216–2.5 is fairly massive and relatively nearby. The integrated *IRAS* flux over the whole cloud is less than $5000 L_{\odot}$, far less than an O or B star. Thus, although there may be a small amount of low-mass star formation within the cloud (see § 2.2. and Lee 1992), G216–2.5 remains the only high-mass cloud for which the existence of O and B stars within its molecular borders can be categorically ruled out. The two scenarios that have been invoked to explain this unusual cloud place it at opposite evolutionary extremes: is it young and unevolved, or is it an old burnt out remnant?

Molecular clouds form from atomic clouds and are always found to be associated with a substantial atomic envelope (Wannier et al. 1991; Andersson & Wannier 1993; Blitz 1993; Kuchar & Bania 1993; Reach, Koo, & Heiles, 1994). The stars that form in molecular clouds, however, will dissociate and ionize their surroundings, eventually returning some fraction of the molecular material to atomic form. Observations of the atomic gas in the vicinity of G216–2.5, therefore, may be a better signature of its evolutionary status, whether very young or very old. The maps of the atomic, molecular, and stellar components in the cloud neighborhood that are presented in this paper suggest that G216–2.5 is a part of a larger molecular complex that has been partially photodissociated by two small OB associations approximately 50 pc from the cloud boundaries. The observations are outlined in § 2, and cloud masses and dissociation rates calculated in § 3. Arguments concerning the evolutionary state of this cloud, and the implications of this

¹ Present address: Center for Astrophysics, MS42, 60 Garden Street, Cambridge, MA 02138; jpw@cfa.harvard.edu.

² Operated by Associated Universities, Inc., under cooperative agreement with the National Science Foundation.

study for molecular cloud evolution and star formation in general, are discussed in § 4. We conclude in § 5.

2. OBSERVATIONS

2.1. Atomic and Molecular Gas

In this work, observations of H I at 21 cm, CO at 2.6 mm, and *IRAS* measurements at 60 and 100 μm are combined to produce an overall picture of the cloud. The CO $J = 1 \rightarrow 0$ observations were made by Maddalena & Thaddeus (1985) using the 1.2 m Columbia telescope. Details of the observational technique are contained in Paper I.

The H I observations were taken in 1989 with the NRAO³ 43 m telescope, which has, at the observed frequency (1420.41 MHz), a beamwidth of 21' and a pointing accuracy of about 30". The observations extend from $l = 212^\circ$ to 220° , $b = -6^\circ$ to 1° and were taken by slewing the telescope in Galactic longitude while taking spectra. Spectra were taken with a spacing of 10' and an integration time of 20 s. The HFET receiver had a typical system temperature of 20 K. We observed both circular polarizations with a 1024-channel autocorrelation back end using a bandwidth of 2.5 MHz and a 1.03 km s^{-1} velocity spacing. After averaging both polarizations, the rms in each spectra is about 0.05 K. The spatial and velocity resolution of the H I observations are well matched to that of the CO (8.8 and 0.65 km s^{-1} , respectively).

The H I spectra were corrected for atmospheric attenuation and, using observations of S8, a standard H I region, scaled to the brightness intensity scale of Williams (1973). We did not correct our data for stray radiation and for slewing the telescope while observing, so the fine details of the map may not be as accurate as possible. Nevertheless, our conclusions, since they are based on the large-scale and gross details of the H I data, are unlikely to be affected by these corrections.

The average CO and H I spectra for all the observations are shown in Figure 1. There are three velocity components present in the H I spectrum, corresponding to three spiral arms along this line of sight (Vogt 1976; see also Fig. 4 below). The central component rises and falls at similar velocities to the mean CO spectrum and is most likely associated with G216–2.5. There is a slight offset between the velocity of the CO and H I peaks, and dips that may be due to the greater size of the H I map and large scale velocity gradients across it. For the remainder of this work, we have restricted attention to the H I in the velocity range $v = 16\text{--}38 \text{ km s}^{-1}$, chosen so as to include all of the CO emission and all the H I in the central component.

2.2. Associated O and B Stars

We searched the POSS prints for objects associated with G216–2.5 and found no bright blue stars and only two faint dark nebular regions that lie within the CO contours (as originally noted in Paper I). However, the large distance to the cloud and its location near the Galactic midplane makes an optical search difficult. We next examined *IRAS* skyflux plates of the region and, although no bright sources lie within the molecular cloud boundaries, several are found within a few degrees of it. The contrast is greatest in a ratio map of the 60–100 μm *IRAS* bands, effectively a map of the local dust temperature (e.g., Wood, Myers, & Daugherty

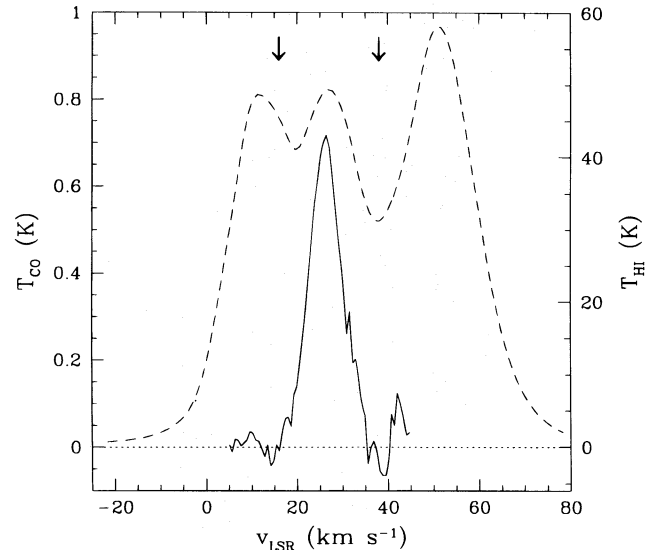


FIG. 1.—Average spectra of H I and CO. The three peaks of the H I correspond to different spiral arms (see Fig. 4). The velocity range, 16–38 km s^{-1} , chosen so as to include all the CO and H I emission associated with the cloud, is indicated by the arrows at the top of the figure.

1994). Figure 2 is a map of the ratio, $R = F_{60}/F_{100}$, overlaid with contours of CO. The exact relation between R and the dust temperature is not of concern here, only that any luminous sources will heat the dust in their neighborhood, thereby signaling their presence in this map.

Indeed, many H II regions stand out in this ratio map; the majority have been cataloged by Sharpless (1959) and are labelled as such in Figure 2. Fich & Blitz (1984) have searched for CO emission toward these objects and measured the velocity of any accompanying CO emission. S284, S285, and S286 all have velocities $v > 45 \text{ km s}^{-1}$ and therefore lie in the more distant spiral arm, beyond G216–2.5. S289 is not a strong *IRAS* source, and no CO was detected toward it, so its velocity (and possible association or lack thereof) is unknown. The velocity of CO emission associated with S287 is 27.2 km s^{-1} , almost identical to the average velocity of G216–2.5. The kinematical distances to these two objects, therefore, is very similar.

There are a number of other sources in the *IRAS* map that are not in the Sharpless catalog. Several are scattered about the edges of the cloud, but, curiously, none lie toward its center. To determine whether these might also be sites of star formation, we have, in the same manner as for the Rosette molecular cloud (Williams, Blitz, & Stark 1995), checked the *IRAS* Point-Source Catalog. We adopt the criteria of Wouterloot et al. (1990) and Wouterloot & Walmsley (1986), which requires that there be firm detections in the 25, 60, and 100 μm bands, that the flux at 25 μm be greater than at 12 μm , and that the colors satisfy

$$0 < R_{23} < 1.5,$$

$$-1 < R_{34} < 0.261 + 0.227R_{23},$$

where $R_{ij} = \log_{10}(v_j S_j / v_i S_i)$ and $i = 1, 2, 3, 4$ corresponds to $\lambda = 12, 25, 60, 100 \mu\text{m}$, respectively. There are four sources that lie within the H I mapped area, satisfy the above criteria, and, at an assumed distance to the cloud of 2.3 kpc (see § 3), have luminosities, $L_{\text{IR}} > 10^3 L_{\odot}$. One is found to coincide with S286, which we have rejected as being associated with G216–2.5 on account of its high radial velocity. Two are found to belong to a young cluster,

³ The National Radio Astronomy Observatory is operated by Associated Universities, Inc., under contract with the National Science Foundation.

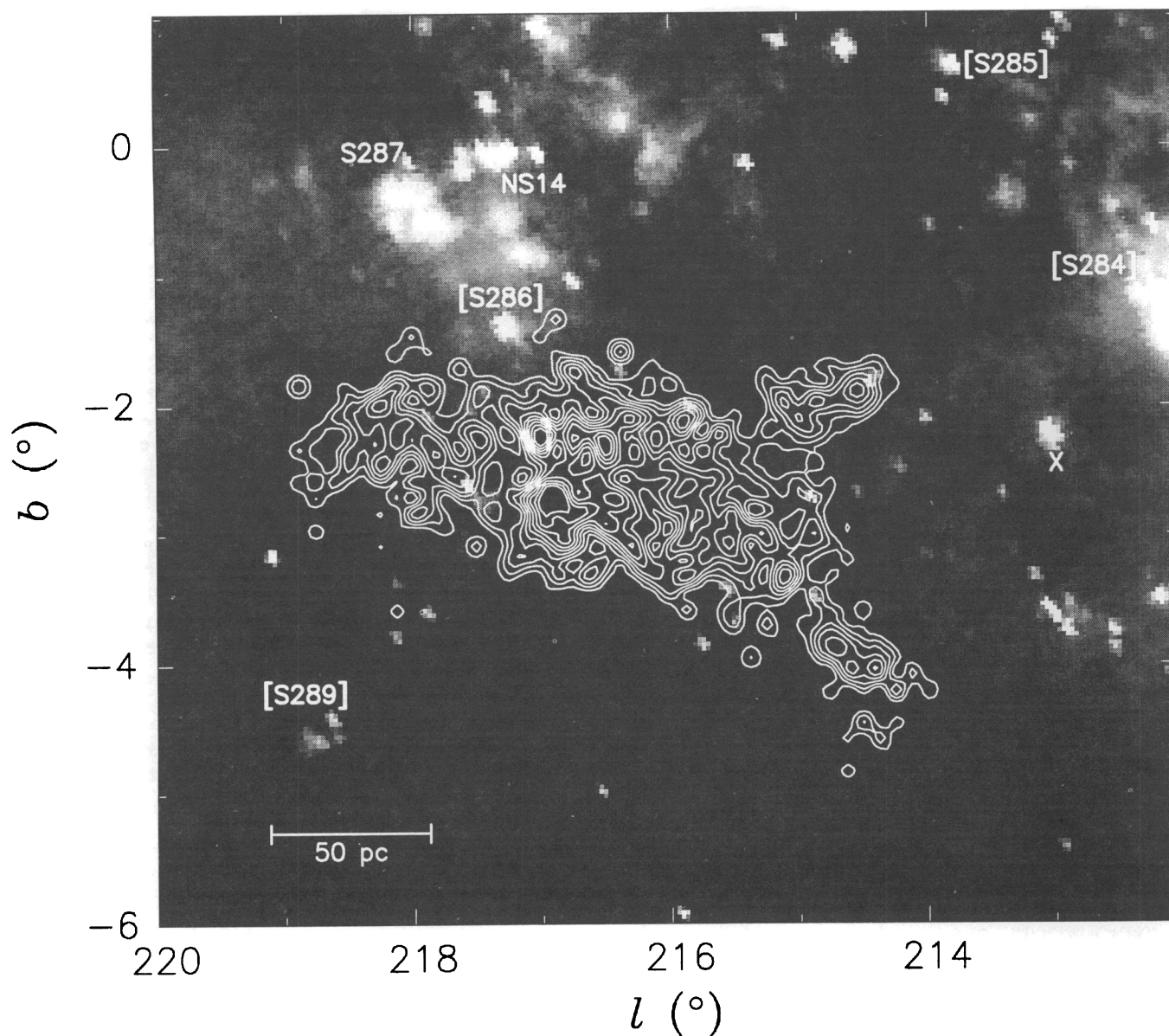


FIG. 2.—*IRAS* flux ratio map in the neighborhood of G216-2.5. The halftone is the ratio of *IRAS* 60–100 μm flux and ranges from 0.08 to 2.6. The highest values of the ratio indicate heated dust and signal the presence of dust-enshrouded stars. Many of the brightest objects are Sharpless H II regions and have been labeled in the diagram. Those with square brackets are at a different velocity than G216-2.5 and therefore not associated. S287 is the only Sharpless object that is at the same velocity as G216-2.5. The two other objects that are labeled are NS 14, an embedded cluster in the S287 cloud, and a source, labeled “X”, at $l = 213^{\circ}07$, $b = -2^{\circ}23$, whose identity is unknown (see text). The contours are of velocity-integrated ($v = 16\text{--}38 \text{ km s}^{-1}$) CO and are at 2, 4, 6, ... K km s^{-1} .

NS 14, of B and A stars embedded in the S287 cloud, studied in detail by Neckel et al. (1989) and Neckel & Staude (1992). There is no information in the literature as to the nature of the remaining source; if at 2.3 kpc, it has an infrared luminosity of $1.1 \times 10^4 L_{\odot}$ (that of a B1 V star; Vacca, Garmany, & Shull 1996) and appears as a small

patch of nebulosity in an image from the digital sky survey.⁴ The *IRAS* fluxes of this object are listed in Table 1 and graphed in Figure 3 against those of NS 14. The similar spectral shapes strongly suggest that this object, labeled “X” in Figure 2 and hereafter referred to in the text as

TABLE 1
IRAS FLUXES OF UNIDENTIFIED POINT SOURCE

l	b	F_{12} (Jy)	F_{25} (Jy)	F_{60} (Jy)	F_{100} (Jy)
213°066.....	-2°228	13.9	159.1	612.0	532.6

⁴ Based on photographic data obtained using the UK Schmidt Telescope. The UK Schmidt Telescope was operated by the Royal Observatory Edinburgh, with funding from the UK Science and Engineering Research Council, until 1988 June and thereafter by the Anglo-Australian Observatory. Original plate material is copyright the Royal Observatory Edinburgh and the Anglo-Australian Observatory. The plates were processed into the present compressed digital form with their permission. The Digitized Sky Survey was produced at the Space Telescope Science Institute under US Government grant NAG W-2166.

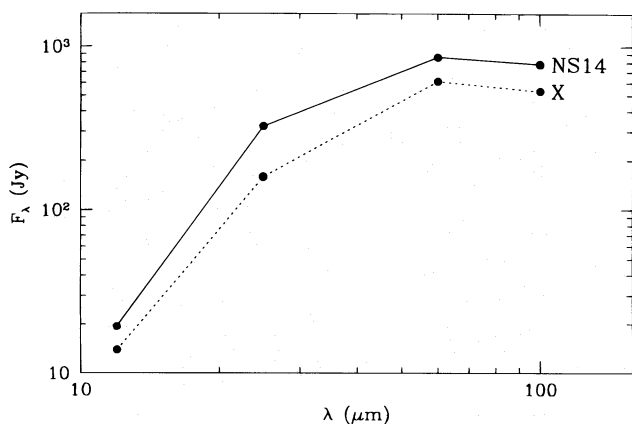


FIG. 3.—Far-infrared spectra (from the *IRAS* Point-Source Catalog) of NS 14 and the unidentified source X in Fig. 2. The similar spectral shapes suggest that source X, like NS 14, is an embedded cluster of recently formed stars.

source X, is also an embedded H II region. The importance of source X to the interpretation of G216–2.5 discussed here warrants more detailed observations to determine its spectral classification and distance.

3. RESULTS

3.1. A Giant Photodissociation Region

Three slices through the CO and H I data cubes are shown in Figure 4. The velocity-integrated plot shows that, although there is no CO emission between either S287 or source X and G216–2.5, there is excess H I emission above a general background level that forms a bridge between them. Particularly at $l \approx 214^\circ$, the morphologies of the CO and H I emission follow each other quite closely, suggesting that this arrangement is not purely coincidental.

The two velocity slices provide further evidence for the close relationship between the molecular gas, the atomic gas, and the regions of star formation. The latitude-integrated plot shows that G216–2.5 lies fully within, and follows the velocity pattern of, the second H I spiral arm. The longitude-integrated plot also shows how the CO, H I, and S287 share the same radial velocity, while demonstrating the spatial offset between them. Unfortunately, since the radial velocity of source X is unknown, it cannot be placed in these diagrams.

It should be pointed out that, at the longitude and distance of G216–2.5, kinematic distances are quite sensitive to radial velocity (≈ 100 pc for a 1 km s^{-1} change in v_r), and the dispersions of the CO and H I are large. By itself, then, any one of these figures does not prove that the atomic and molecular gas are physically associated. Taken together, however, the three figures, showing the full l - b - v relation between the two data sets, are far less likely to be merely a chance alignment and make a compelling case for a causal relation between the molecular gas, the atomic gas, and the site(s) of star formation.

We propose and will attempt to prove that the H I emission in the vicinity of G216–2.5 is photodissociated gas resulting from star formation in the surrounding molecular complex. Under this interpretation, the atomic gas can be considered a giant low-density photodissociation region (Hollenbach, Takahashi, & Tielens 1991), some 50 pc wide and several hundred parsecs in length.

3.2. Mass Estimates

3.2.1. Molecular Mass

The molecular mass of the cloud was calculated in Paper I to be $6.6 \times 10^5 M_\odot$ assuming a (kinematic) distance to G216–2.5 of 3 kpc. Based on a flat rotation curve with a circular velocity $\theta_0 = 220 \text{ km s}^{-1}$, Galactocentric distance $R_0 = 8.5 \text{ kpc}$, and a dispersion velocity for the gas of 7 km s^{-1} , the kinematic distance to G216–2.5 is $2.6 \pm 0.8 \text{ kpc}$. Distances quoted in the literature vary from 2.3 to 3.2 kpc. Since the derived CO mass of the cloud is proportional to the square of the distance, the uncertainty in the latter results in uncertainties in the mass of up to 70%. However, under the assumption that G216–2.5 is associated with S287 and stars of known spectral type in the S287 cloud, the distance to G216–2.5 can be more firmly established photometrically to be 2.3 kpc (Neckel et al. 1989). This is also in good agreement with an observed jump in the reddening of bright stars at 2.2 kpc toward G216–2.5 (Lee et al. 1991). For the remainder of this paper, we assume a distance to G216–2.5 of 2.3 kpc.

After correcting for a closer distance of 2.3 kpc and a more recent value for the conversion factor, $N_{\text{H}_2}/W_{\text{CO}} = 2.3 \times 10^{20} \text{ cm}^{-2} \text{ K}^{-1} \text{ km s}^{-1}$ (Bloemen 1989), we arrive at a mass $M_{\text{mol}} = 3.4 \times 10^5 M_\odot$. This is in good agreement with the CO mass of the cloud derived by Lee et al. (1994) from FCRAO observations.

It is worth noting that with the revised, closer distance to G216–2.5, it is one of the most massive molecular clouds in the solar neighborhood. Its overall mass is even higher when the mass of associated H I and surrounding molecular material (see § 4.) is taken into account.

3.2.2. Atomic Mass

Estimating the mass of atomic gas associated with G216–2.5 is made difficult by the ubiquity of H I emission along all lines of sight to the cloud, and a consequent ambiguity about the precise amount of H I that is associated with it. On the other hand, however, the ubiquity of emission implies that any unassociated H I emission tends to be rather smoothly distributed and can be considered as a mostly uniform background level. We have clipped the H I data, made maps at a variety of background levels, and find that there is excess H I column density in the vicinity of G216–2.5, and in the same velocity range, however high the clipping. We attribute this excess emission as being associated atomic gas with the molecular cloud. By subtracting out the background and summing up the excess emission, we can determine its mass.

As an example, Figure 2 shows the excess emission above a background level $N_{\text{H I, back}} = 2.0 \times 10^{21} \text{ cm}^{-2}$; 624 pointings (out of a total of 2064) exceed this level and cover an area $A_{\text{H I, excess}} = 2.8 \times 10^4 \text{ pc}^2$. The average $N_{\text{H I}}$ of the emission in this area is $2.21 \times 10^{21} \text{ cm}^{-2}$, which is greater than the background level by an amount $N_{\text{H I, excess}} = 2.1 \times 10^{20} \text{ cm}^{-2}$. The mass of the atomic cloud is this excess column integrated over $A_{\text{H I, excess}}$ and is equal to $M_{\text{atm}} = 6.4 \times 10^4 M_\odot$ (including a factor of 1.36 for Helium).

Similar calculations have been performed for a variety of background levels to show its effect on the atomic mass estimate. The results are graphed in Figure 5. As $N_{\text{H I, back}}$ decreases, both $A_{\text{H I, excess}}$ and $N_{\text{H I, excess}}$ increase, implying a very rapid increase in M_{atm} . Eventually, at $N_{\text{H I, back}} = 0.6 \times 10^{21} \text{ cm}^{-2}$, $A_{\text{H I, excess}}$ saturates to that of the entire mapped region, but M_{atm} continues to increase because

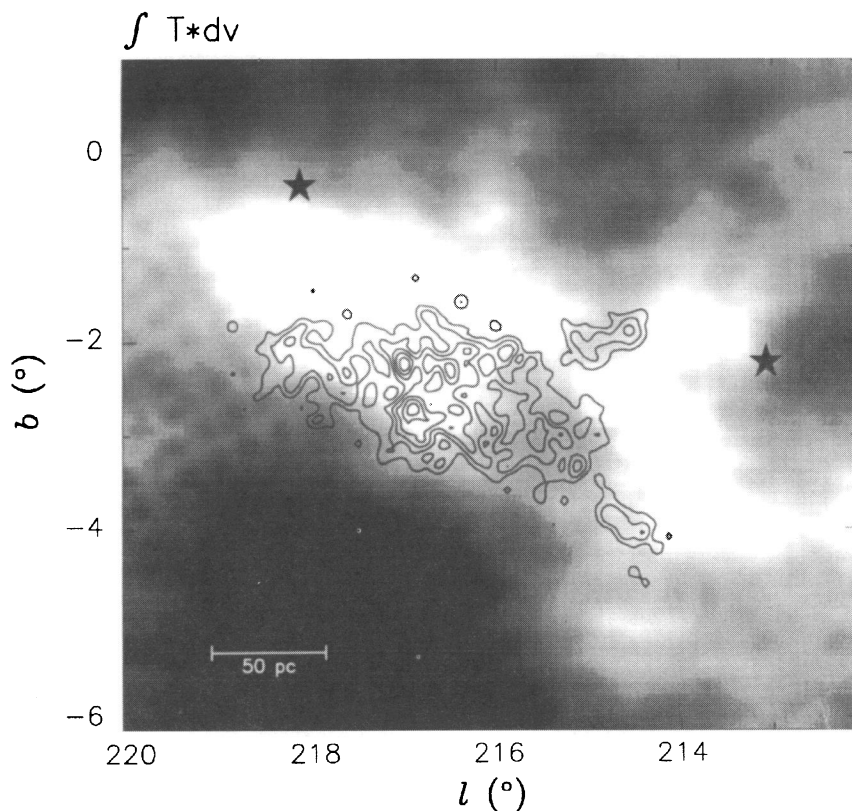


FIG. 4a

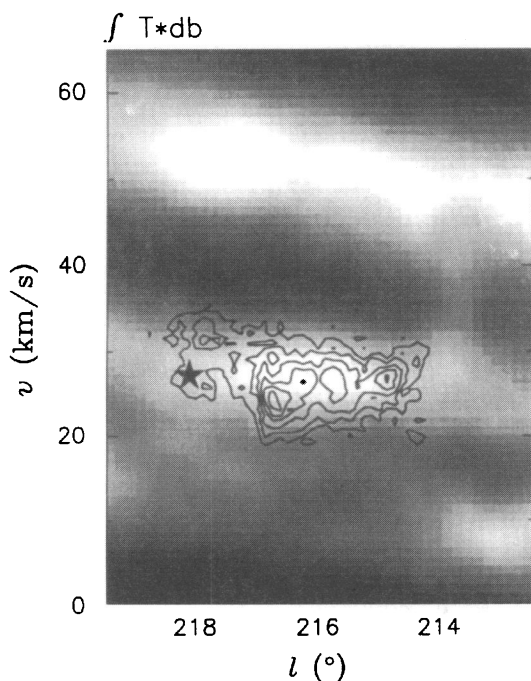


FIG. 4b

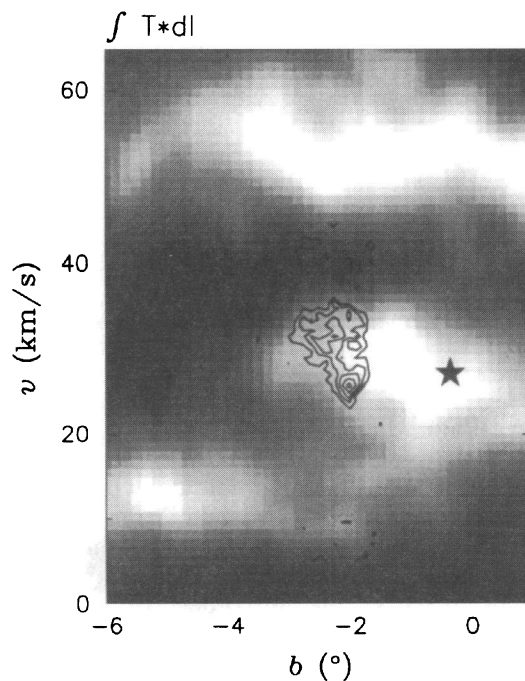


FIG. 4c

FIG. 4.— l - b - v relationship between the molecular and atomic gas. Three projections through the data cubes, along the velocity, latitude, and longitude axes, respectively, are shown. In each case the H I emission is shown in gray scale, the CO in contours, and S287 by the star-shaped symbol. (a) l - b plot integrated from $v = 16$ – 38 km s^{-1} ; contours are at 4, 8, 12, ... K km s^{-1} , and the gray scale ranges from 1.8 to $2.8 \times 10^{21} \text{ cm}^{-2}$. The second star-shaped symbol at $l = 213^\circ$, $b = -2.2^\circ$ shows the location of source X. The CO contours have been deliberately chosen to be twice as high as in Fig. 2 in order to show the fragmented appearance of the molecular gas closest to S287 and source X. (b) l - v plot integrated from $b = -4^\circ$ to -1° ; contours are at 0.2, 0.4, 0.6, ... deg K, and the gray scale ranges from 36° to 360° K . Three spiral arms can be seen in the H I, and the velocities of the CO and the second H I spiral arm follow each other closely. (c) b - v plot integrated from $l = 217.8$ to 218.4 ; contours are at 0.1, 0.2, 0.3, ... deg K, and the gray scale ranges from 6° to 60° K . The velocity coincidences, but spatial offsets, between the CO, H I, and S287, are clearly visible. Together, these three plots demonstrate that the CO, H I, and S287 are all spatially and kinematically associated; it is unlikely that such a close alignment in all three axes as seen here can be purely coincidental.

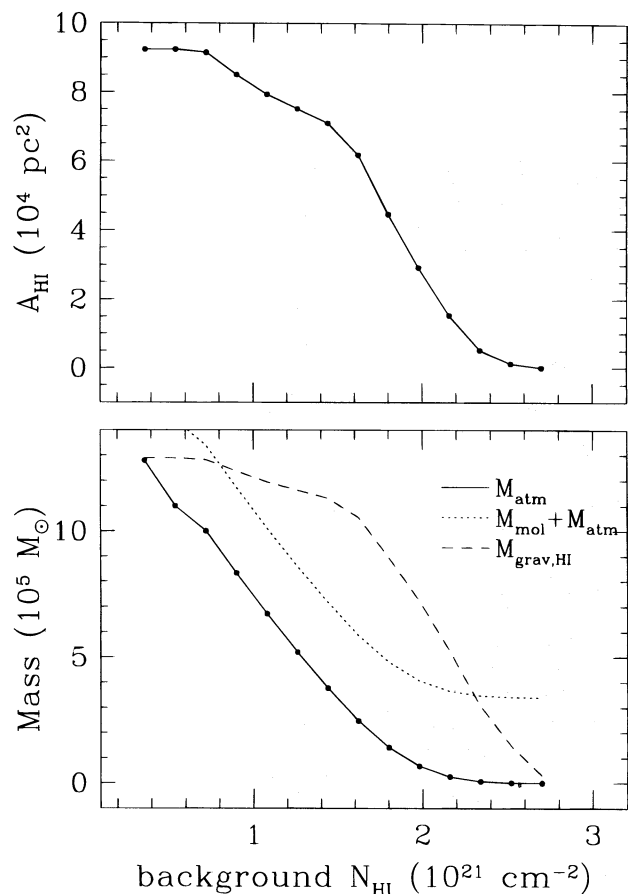


FIG. 5.—Variation of atomic area and mass determinations on the assumed uniform background level of H I toward the cloud. The H I emission is integrated over the velocity range of the cloud, $v = 16\text{--}38 \text{ km s}^{-1}$, and a background column density (abscissa) is subtracted. The excess emission is attributed to the cloud, and its mass and area calculated in the manner described in the text. The total (molecular plus atomic) mass of the G216–2.5 complex and a lower limit to the combined gravitational mass are also shown.

$N_{\text{HI,excess}}$ is still increasing. There is a very wide range, $\sim 10^4$ to $\sim 10^6 M_{\odot}$, in the possible values for M_{atm} , and its exact value may be very uncertain if the background level, $N_{\text{HI,back}}$, is high, for then $N_{\text{HI,excess}}$ is only a small fraction of the background and very sensitive to very small changes in it. In the above example in Figure 2, for example, decreasing $N_{\text{HI,back}}$ by 10% almost doubles the value of $N_{\text{HI,excess}}$.

As discussed in the introduction, molecular clouds are observed to be embedded in a larger atomic cloud that may be a remnant of their formation or a shield against dissociating photons in the general interstellar radiation field. Typical column densities of associated H I around giant molecular clouds (GMCs) are of order 10^{21} cm^{-2} (Andersson & Wannier 1993; Kuchar & Bania 1993). In the case of G216–2.5, this is attained for $N_{\text{HI,back}} \simeq 0.8 \times 10^{21} \text{ cm}^{-2}$, which implies $M_{\text{atm}} \simeq 10^6 M_{\odot}$, a very large cloud. At this background level, almost all lines of sight contribute some excess emission, and the associated cloud is at least as large as the mapped area. The large-scale H I survey of Weaver & Williams (1974) shows that G216–2.5 appears to sit at the southern end of a large H I cloud that extends to $b \gtrsim 2^{\circ}$.

In Figure 2, a high background level, $N_{\text{HI,back}}$, was deliberately chosen so as to highlight any excess H I that may be

due to more localized photodissociation sources above a larger, more symmetrically distributed, cloud envelope. Since the mass of this excess is calculated to be only a small fraction, $\simeq 10\%$ of the postulated envelope, the amount of local photodissociation would appear to be rather small (§ 3.3).

3.2.3. Gravitational Mass

The gravitational mass of G216–2.5 may be determined from its size, $R_{\text{CO}} = (A_{\text{CO}}/\pi)^{1/2} = 55 \text{ pc}$, and line width, $\Delta V_{\text{CO}} = 8.5 \text{ km s}^{-1}$ (Paper I). Assuming a uniform, spherical cloud, the gravitational mass is $M_{\text{grav}} = 5R\sigma_v^2/2G = 4.2 \times 10^5 M_{\odot}$, where $\sigma_v = \Delta v/2.355$ is the velocity dispersion. Estimates of this type are quite uncertain, but since $M_{\text{grav}} \simeq M_{\text{mol}}$, the kinetic energy of the cloud, $T = 3M\sigma_v^2/2$, is in approximate balance with its gravitational potential energy, $|V| = 3GM^2/5R$, and the cloud is marginally stable. Lee et al. (1994) came to the opposite conclusion based on a lower mass for the cloud derived from their ^{13}CO measurements. We believe, however, that this mass may be an underestimate of the total molecular mass because of the low ^{13}CO peak brightness temperatures in the cloud and the limited sensitivity of their observations. The cloud mass that they derive from their own CO measurements does agree with ours and is almost a factor of 3 greater than their ^{13}CO -derived mass.

The gravitational mass of the atomic gas associated with G216–2.5 is harder to ascertain. This is because of the background problem mentioned above, which implies an uncertainty in the total mass and size of the H I cloud, and also an uncertainty in its line width. It is not known how much H I is associated with G216–2.5 at any given velocity, and therefore an average spectrum of the associated atomic cloud is difficult to determine. Nevertheless, the velocity dispersion of the molecular gas places a lower bound on that of the H I, $\sigma_v = 3.6 \text{ km s}^{-1}$, which can be used with the cloud area from the upper panel of Figure 5 to calculate a lower limit to the gravitational mass. This lower limit is plotted, as a function of $N_{\text{HI,back}}$, in the lower panel in Figure 5. The gravitational mass of the atomic cloud exceeds, by a wide margin, its luminous mass at all but the lowest background levels. At these low levels, the H I cloud fills almost the entire map and only a lower limit to its size can be measured. Also in this case, the cloud is so large that its H I velocity dispersion is likely to be much greater than that of the CO, and its virial mass is therefore much larger than Figure 5 indicates. By itself, therefore, the atomic cloud (whatever its mass) does not appear to be self-gravitating. This may be caused by the process of dissociation itself, which increases the specific kinetic energy of the dissociated atomic gas relative to the molecular gas (Black & Dalgarno 1977).

Is the atomic gas bound to the molecular cloud? The total mass of the system, $M_{\text{tot}} = M_{\text{mol}} + M_{\text{atm}}$, is also plotted in Figure 5. The gravitational mass of the H I alone exceeds M_{tot} for most background levels, and the combined gravitational mass of the system (estimating the size from the total area of CO and H I emission) is greater than M_{tot} at all levels.

We conclude, therefore, that the molecular cloud is marginally gravitationally bound, but that the dissociated atomic gas is unbound, both to itself and to the (molecular plus atomic) system as a whole; it is presumably escaping into the general interstellar medium (ISM).

3.3. The H₂ Dissociation Rate

The identification, and association with G216–2.5, of each of the *IRAS* sources in the field is discussed in § 2.2. S287 is the most likely major source of photodissociation. *UBV* colors have been measured toward this source and match that of an O9.5 V star (Moffat, Fitzgerald, & Jackson 1979), although there may be other B stars in the cluster that could add significantly to the photodissociation rate. The *IRAS* luminosity of this source is far less than the total luminosity of an O9.5 V star, suggesting that it has broken free from any surrounding molecular material and leaving relatively little extinction between it and G216–2.5.

There are several other sites of star formation within the S287 molecular cloud. The brightest in the *IRAS* map is NS 14, a young, embedded cluster of B and A stars studied by Neckel et al. (1989). They estimate that the obscuration around the cluster amounts to $A_V \simeq 6$ mag. We conclude, therefore, that most of the radiation from NS 14 is absorbed locally and its contribution to the dissociating flux at the surface of G216–2.5 is negligible.

The morphology of the H I and CO contours at lower longitudes, $l \simeq 214^\circ$, is also suggestive of dissociation. However, a source responsible for this CO–H I offset is not so immediately apparent as on the other side of the cloud. S284 is at a much higher velocity than G216–2.5 and probably lies in the more distant spiral arm beyond the cloud. Source X, discussed in § 2.2, has the *IRAS* colors of an embedded H II region and is ideally situated relative to the CO and H I emission, but its identity and distance are unknown. If at the distance of G216–2.5, it has an infrared luminosity of $1.1 \times 10^4 L_\odot$, that of a B1 V star. For the purposes of this discussion, we will assume that the unidentified object is a B1 V star and that it is the sole agent responsible for the dissociated H I cloud on the low-longitude side of the cloud.

Molecular hydrogen is dissociated by far-ultraviolet (FUV) photons in the energy range 11–13.6 eV. The dissociating stars, type O9.5 V and B1 V, have a combined total luminosity $\simeq 10^5 L_\odot$ (Vacca et al. 1996). The distance between the cloud and the stars is at least as great as the projected displacement in Figure 2, ~ 50 pc. The flux at the cloud's surface is therefore no greater than 1.3×10^{-3} ergs $\text{cm}^{-2} \text{s}^{-1}$ and will be lower still with allowance for dust absorption. This is a weak flux, about equal to the mean interstellar radiation field, 1.6×10^{-3} ergs $\text{cm}^{-2} \text{s}^{-1}$ (Habing 1968), implying that the present effect of the stars on G216–2.5 is no greater than that due to the general interstellar field. To explain the observed photodissociation region (PDR), therefore, either the stars were closer to the molecular cloud in the past or there was a previous, more luminous, burst of star formation.

In fact, we must appeal to the latter, since the PDR is too vast to have been created by an O9.5 and B1 star, as can be seen by the following argument. The rate of H₂ dissociation (e.g., de Jong, Dalgarno, & Boland 1980) is

$$R_d = 2 \times 10^{-5} G_0 e^{-2.54\nu} N_{\text{H}_2}^{-1/2} n_{\text{H}_2},$$

where $G_0 \simeq 1$ is the ratio of the incident FUV flux on the cloud to the Habing value. The units of R_d are $\text{cm}^{-3} \text{s}^{-1}$, if N_{H_2} is measured in cm^{-2} and n_{H_2} in cm^{-3} . H₂ is formed by adhesion of H I onto dust grains and occurs at a rate (Spitzer 1978)

$$R_f = \gamma n_{\text{H I}} n_{\text{tot}},$$

where $\gamma \simeq 3 \times 10^{-17} \text{ cm}^3 \text{ s}^{-1}$. These rates will vary throughout the cloud because of inhomogeneities in the gas densities, but since $G_0 \simeq 1$ at the cloud surface, S287 and source X probably maintain the PDR in equilibrium, $R_d \simeq R_f$.

If, however, at earlier times G216–2.5 was larger and there was molecular gas closer to S287 (and source X), the radiation field would be stronger and $R_d \gg R_f$, resulting in dissociation of H₂ at a net rate $dn_{\text{H}_2}/dt = R_f - R_d \simeq -R_d$. Complete dissociation would occur in a time $t_d \simeq n_{\text{H}_2}/R_d$, and independent of n_{H_2} as long as the approximation $R_d \gg R_f$ is valid (for example, if the gas is not strongly clumped, and the stars are sufficiently close to the gas so that the radiation field is not too weak). With these conditions, and ignoring dust absorption, t_d may be determined for any distance, x , from the dissociating stars,

$$t_d(x) \simeq 5 \times 10^4 N_{\text{H}_2}^{1/2}(x) \left(\frac{x}{x_1} \right)^2,$$

where $x_1 \simeq 50$ pc is the distance for which $G_0 = 1$. We can replace $N_{\text{H}_2}(x)$ by $\langle n_{\text{H}_2} \rangle x$, the average volume density times the path length of the gas; this is also relatively insensitive to any clumping of the gas. Therefore, assuming that the original molecular cloud prior to dissociation had the same mean molecular density as is observed now, we arrive at

$$t_d(x) = 45 \left(\frac{x}{50 \text{ pc}} \right)^{5/2} \text{ Myr}.$$

At large distances from the stars, dust absorption becomes significant and the approximation $R_d \gg R_f$ is no longer valid, so the net dissociation rate will be lower and t_d is a lower limit to the time required to dissociate the gas. Since $t_d(50 \text{ pc}) = 45$ Myr, the timescale for these stars to create the observed PDR is much greater than their main-sequence lifetimes, and we conclude that it must have been formed by a previous, more luminous generation of star formation.

4. DISCUSSION

The mass of G216–2.5 is greater than both the Rosette molecular cloud and the Orion A and B clouds, and yet, unlike these clouds, it is not currently forming any massive stars. This paper presents H I observations in the vicinity of G216–2.5 that show that the cloud is associated with at least one, and perhaps two, OB stellar groups over 50 pc away. However, there is no massive star formation occurring within the CO contours themselves; the *IRAS* luminosity-to-cloud mass ratio is extremely low, $L_{\text{IR}}/M_{\text{cloud}} \simeq 0.02 L_\odot/M_\odot$, compared with $\geq 1 L_\odot/M_\odot$ for the Orion and Rosette clouds. In this sense, therefore, G216–2.5 remains a very enigmatic object; any star formation that is presently occurring within the cloud is at a very low level. How do the observations presented here of the cloud's large-scale environment affect the interpretation of its evolutionary state?

4.1. Evidence that G216–2.5 is Young

The original argument for the cloud's youth remains the strongest one: that there is no current star formation within its boundaries. The *IRAS* maps, and more sensitive studies by Lee (1992), confirm the lack of massive star formation

within the cloud but find a small number of embedded low-mass star-forming regions scattered around its edges. The cloud, therefore, must be at least a few Myr old, but these observations may actually strengthen the case that the cloud is young: an evolved cloud of this mass should be riddled with stars. The luminosity-to-mass ratio is exceptionally low even compared with such low-mass star-forming clouds as Taurus (Kenyon et al. 1990).

The average column density of G216–2.5 is $1.5 \times 10^{21} \text{ cm}^{-2}$, significantly less than that of the Rosette ($4 \times 10^{21} \text{ cm}^{-2}$; Williams et al. 1995) or Orion ($3 \times 10^{21} \text{ cm}^{-2}$; Maddalena et al. 1986) molecular clouds, and more typical of low-mass star-forming clouds such as Taurus (Ungerechts & Thaddeus 1987). Its linear dimensions, however, are very much larger than typical star-forming GMCs, and it may be described as a large, low surface brightness cloud, such as would be expected for a young cloud prior to forming stars in the photoionization regulated star formation model of McKee (1989).

The H I observations here clearly demonstrate the association of G216–2.5 with S287 (and possibly with the unidentified source X), but they are too far away, and insufficiently luminous, to have any significant effect on the molecular gas. Figures 2 and 4 may not, therefore, contradict the picture of a relatively isolated cloud undergoing gravitational contraction prior to star formation.

4.2. Evidence that G216–2.5 is Old

Lee et al. (1994) have presented several arguments that suggest the cloud is old and evolved, based on its large line width, gravitational imbalance, and disturbed small-scale and large-scale kinematics.

The cloud line width, $\Delta V = 8.5 \text{ km s}^{-1}$, is slightly larger than the Orion or Rosette GMCs, for instance, but its mass is several times larger. We find that the cloud is in approximate gravitational balance, $M_{\text{mol}} \simeq M_{\text{grav}}$. The discrepancy with the Lee et al. result is believed to be due to the low sensitivity of their ^{13}CO observations to all the gas in the cloud.

There are several rings and shells that are clearly visible in their high-resolution maps, but no optical counterparts that might be responsible for their formation are found. Dynamical ages of the order of several Myr are inferred, which places a lower limit to the cloud's age. However, the overall velocity pattern across the whole cloud (Fig. 9 of Lee et al. 1994) is, perhaps, stronger evidence for an interaction with a previous energetic burst of star formation. Additional morphological evidence for disruption of the cloud is shown in the velocity-integrated map in Figure 4, which appears to show that the CO emission is most fragmented closest to the postulated dissociating sources.

The association of G216–2.5 with S287 (and possibly source X) that is shown in the H I data certainly testifies to a more active, star-forming, history in this region. There are also several published maps that show additional molecular gas in the vicinity of G216–2.5; Figure 2 of Paper I (see also May et al. 1993; May, Murphy, & Thaddeus 1988) shows that there are many small fragments of molecular gas at the same velocity as, and in close proximity to, G216–2.5. Taken together, these observations suggest that G216–2.5 is part of a large, massive star-forming, molecular complex. As we have argued above, however, this does not conclusively prove that G216–2.5 is an old remnant. It is possible, for instance, that one side of a cloud may still be

condensing out of the diffuse ISM as the other side forms stars (Elmegreen & Lada 1977).

The principal difficulty with the assumption of an old age for the cloud is explaining the lack of star formation within it. G216–2.5 is very massive, and there are several clumps with masses $\gtrsim 10^3 M_{\odot}$ in the central part of the cloud (Williams et al. 1994). However, unlike clumps in star-forming GMCs (Bertoldi & McKee 1992), even the most massive clumps in G216–2.5 are gravitationally unbound, yet, in the Rosette molecular cloud, Williams et al. (1995) found that boundedness of the clumps was a prerequisite for massive star formation. In this sense, therefore, the dynamics of the internal structure of G216–2.5 is consistent with its lack of massive star formation, although it is unclear how such relatively high-velocity dispersions in the clumps, and the cloud as a whole, can be maintained without stellar energy input. It was shown in § 3.3 that any present effect of the massive star formation sites in the vicinity of G216–2.5 is small.

If G216–2.5 is a remnant cloud, therefore, one might expect to find more luminous associated stars (or evidence of their supernovae) in its neighborhood. Such evidence is also required to explain the origin of the observed PDR. However, no pulsars in the cloud's neighborhood are found in the catalog of Taylor, Manchester, & Lyne (1993), and there are no strong radio continuum sources that appear to be associated with the cloud in the surveys at 408, 1420, and 4850 MHz (Haslam et al. 1982; Reich 1982; Condon, Broderick, & Seielstad 1991, respectively).

4.3. How Common is G216–2.5?

There are strong arguments on both sides for an old or a young cloud. If it is young, its location in an apparently fragmented star-forming complex should be understood. If it is old, evidence for a previous generation of very luminous star formation should be found (cf. Elmegreen 1991). Regardless of its age, however, it is clear that G216–2.5 is in a very different evolutionary state than, for example, the Orion or Rosette molecular clouds. How common is such a cloud?

Although G216–2.5 is unlike any other molecular cloud that has been observed in detail in the solar neighborhood, similar clouds to the one described here might be expected to be rather common (although possibly in less extreme evolutionary states). Mooney & Solomon (1988) found that 60% of the clouds in their Galactic survey were “cold” and not associated with bright H II regions. Similarly, Chiar et al. (1994) and Brand & Wouterloot (1995) have argued, also based on observations of low brightness temperature CO lines, for the existence of G216–2.5-like objects in, respectively, the inner and outer Galaxy. It is worth pointing out, however, that in the above three studies, the clouds that the authors found are generally less massive than G216–2.5, are much farther away, and observed at far poorer resolution. It is not yet possible, from these studies alone, to conclude that there exists a large number of massive ($\gtrsim 10^5 M_{\odot}$) molecular clouds that are not forming OB stars in the Galaxy.

On the other hand, not all GMCs can contain bright associations such as the Orion or Rosette clouds. A count of the numbers of OB associations and GMCs in the Galaxy by Williams & McKee (1996) shows that the likelihood that a $10^5 M_{\odot}$ molecular cloud contains an association as luminous as the Orion nebula is only about 20%; such clouds

are far more likely to contain only a single O9 star or just B stars (e.g., the Vela molecular clouds; Liseau et al. 1992). The star-forming molecular complex that G216–2.5 belongs to, therefore, may be rather typical in the Galaxy. The complete absence of massive star formation in the cloud itself, however, appears to be quite unusual.

5. CONCLUSION

An associated neutral atomic cloud has been found around the G216–2.5 molecular cloud. The spatial coincidence and similar kinematics of the H I and CO suggest that the molecular gas is linked by an atomic bridge, with a projected width of 50 pc, to two regions of OB star formation. We conclude, therefore, that, although G216–2.5 is not currently forming massive stars, it is a part of a larger star-forming molecular complex.

The mass of atomic gas is difficult to estimate because the background column density of unassociated gas along the line of sight is large and unknown. If G216–2.5 has an atomic envelope around it with a column, $N_{\text{HI}} \simeq 10^{21} \text{ cm}^{-2}$, typical of other GMCs, then the total mass of associated H I is of order $10^6 M_{\odot}$. The postulated atomic bridge mapped in Figure 4 is at an even higher column density and is an excess over the general cloud envelope, which is presumed more uniform and symmetric. The mass of this excess H I is of order $10^5 M_{\odot}$ but is highly uncertain and may be in error by at least a factor of 2. Nevertheless, whatever the mass of H I, it seems to be unbound both to itself and to the molecular complex and may be evaporating into the general ISM.

The two stellar groups that appear to be associated with G216–2.5 are S287 and an unidentified IRAS point source with the colors of an embedded H II region. The luminosity of S287 is dominated by a single O9.5 V star, and the unidentified source has an infrared luminosity, $L_{\text{IR}} = 1.1 \times 10^4 L_{\odot}$ (equal to that of a B1 V star). At a minimum distance of 50 pc from G216–2.5, their effect on the molec-

ular gas is small. The total flux on the cloud due to the stars in these H II regions probably amounts to no more than the Galactic average Habing field, and it is suggested that the excess H I that is seen between G216–2.5 and the stars is an equilibrium PDR for which the H_2 dissociation rate balances the H_2 formation rate.

The origin of the PDR, however, has not been explained. If the atomic cloud is truly associated with G216–2.5, it must have been created by a previous generation of luminous star formation and is now only being maintained in equilibrium by S287 and the unidentified source X. Nevertheless, despite this uncertainty, with a width on the sky of more than a degree, this PDR is an excellent laboratory in which to observe the chemistry in such regions and the details of the transition from atomic to molecular gas.

The H I observations do not necessarily contradict the original suggestion in Paper I that the cloud is young and unevolved since the stars are so far away that their present effect on the molecular gas is minor. On the other hand, it adds weight to the assertion by Lee et al. (1994) that the cloud is an old remnant of a star-forming molecular complex. However, the reason why such a large mass of molecular gas is not currently forming OB stars, or substantial numbers of any types of stars, is still not understood.

We would like to thank Bill Vacca for communicating results prior to publication. This work has made use of data obtained through the High Energy Astrophysics Science Archive Research Center Online Service, provided by the NASA/Goddard Space Flight Center, and the SIMBAD database operated at CDS, Strasbourg, France. Many informative discussions with Leo Blitz, Eugène de Geus, Tom Dame, Carl Heiles, Chris McKee, and Phil Myers are gratefully acknowledged. This work was supported, in part, by NSF grant NSF-FD93-20238.

REFERENCES

- Andersson, B.-G., & Wannier, P. G. 1993, *ApJ*, 402, 585
 Bertoldi, F., & McKee, C. F. 1992, *ApJ*, 395, 140
 Black, J. H., & Dalgarno, A. 1977, *ApJS*, 34, 405
 Blitz, L. 1993, in *Protostars and Planets III*, ed. E. H. Levy & J. I. Lunine (Tucson: Univ. Arizona Press), 125
 Bloemen, J. B. G. M. 1989, *AR&A*, 27, 469
 Brand, J., & Wouterloot, J. G. A. 1995, *A&A*, 303, 851
 Chiar, J. E., Kutner, M. L., Verter, F., & Leous, J. 1994, *ApJ*, 431, 658
 Condon, J. J., Broderick, J. J., & Seielstad, G. A. 1991, *AJ*, 102, 2041
 de Jong, T., Dalgarno, A., & Boland, W. 1980, *A&A*, 91, 68
 Elmegreen, B. G. 1991, in *The Physics of Star Formation and Early Stellar Evolution*, ed. C. J. Lada & N. D. Kylafis (Dordrecht: Kluwer), 35
 Elmegreen, B. G., & Lada, C. J. 1977, *ApJ*, 214, 725
 Fich, M., & Blitz, L. 1984, *ApJ*, 279, 125
 Habing, H. J. 1968, *Bull. Astron. Inst. Netherlands*, 19, 421
 Haslam, C. G. T., Salter, C. J., Stoffel, H., & Wilson, W. E. 1982, *A&AS*, 47, 1
 Hollenbach, D. J., Takahashi, T., & Tielens, A. G. G. M. 1991, *ApJ*, 377, 192
 Kenyon, S. J., Hartmann, L. W., Strom, K. W., & Strom, S. E. 1990, *AJ*, 99, 869
 Kuchar, T. A., & Bania, T. M. 1993, *ApJ*, 414, 664
 Lee, Y. 1992, Ph.D. thesis, Univ. Massachusetts, Amherst
 Lee, Y., Snell, R. L., & Dickman, R. L. 1991, *ApJ*, 379, 639
 ———. 1994, *ApJ*, 432, 167
 Liseau, R., Lorenzetti, D., Nisini, B., Spinoglio, L., & Moneti, A. 1992, *A&A*, 265, 577
 Maddalena, R., Morris, M., Moscowitz, J., & Thaddeus, P. 1986, *ApJ*, 303, 375
 Maddalena, R., & Thaddeus, P. 1985, *ApJ*, 294, 231 (Paper I)
 May, J., Bronfman, L., Alvarez, H., Murphy, D. C., & Thaddeus, P. 1993, *A&AS*, 99, 105
 May, J., Murphy, D. C., & Thaddeus, P. 1988, *A&AS*, 73, 51
 McKee, C. F. 1989, *ApJ*, 345, 782
 Moffat, A. F. J., Fitzgerald, M. P., & Jackson, P. D. 1979, *A&AS*, 38, 197
 Mooney, T. J., & Solomon, P. M. 1988, *ApJ*, 334, L51
 Myers, P. C., Dame, T. M., Thaddeus, P., Cohen, R. S., Silverberg, R. F., Dwek, E., & Hauser, M. G. 1986, *ApJ*, 301, 398
 Neckel, T., & Staude, H. J. 1992, *A&A*, 254, 339
 Neckel, T., Staude, H. J., Meisenheimer, K., Chini, R., & Güsten, R. 1989, *A&A*, 210, 378
 Reach, W. T., Koo, B.-C., & Heiles, C. 1994, *ApJ*, 429, 672
 Reich, W. 1982, *A&AS*, 48, 219
 Sharpless, S. 1959, *ApJS*, 4, 257
 Solomon, P. M., Sanders, D., & Rivolo, A. R. 1985, *ApJ*, 219, L19
 Spitzer, L. J. 1978, *Physical Processes in the Interstellar Medium* (New York: Wiley)
 Taylor, J. H., Manchester, R. N., Lyne, A. G. 1993, *ApJS*, 88, 529
 Ungerechts, H., & Thaddeus, P. 1987, *ApJS*, 63, 645
 Vogt, N. 1976, *A&A*, 53, 9
 Vacca, W. D., Gamany, C. D., & Shull, J. M. 1996, *ApJ*, 460, 914
 Wannier, P. G., Andersson, B.-G., Morris, M., & Lichten, S. M. 1991, *ApJS*, 75, 987
 Weaver, H., & Williams, D. R. W. 1974, *A&AS*, 17, 1
 Williams, D. R. W. 1973, *A&AS*, 8, 505
 Williams, J. P., Blitz, L., & Stark, A. A. 1995, *ApJ*, 451, 252
 Williams, J. P., de Geus, E. J., & Blitz, L. 1994, *ApJ*, 428, 693
 Williams, J. P., & McKee, C. F. 1996, *ApJ*, in press
 Wood, D. O. S., Myers, P. C., & Daugherty, D. A. 1994, *ApJS*, 95, 457
 Wouterloot, J. G. A., Brand, J., Burton, W. B., & Kwee, K. K. 1990, *A&A*, 230, 21
 Wouterloot, J. G. A., & Walmsley, C. M. 1986, *A&A*, 168, 237